TRANSACTIONS OF THE INSTITUTE OF FLUID-FLOW MACHINERY

No. 132, 2016, 17–28

Vitaliy Nezym[1]

Aerodynamic test of fixed-geometry and adjustable additional blades in axial-flow compressor stage

National Aerospace University 'Kharkov Aviation Institute',Chkalova 17, Kharkov, 61070, Ukraine

Abstract

An application of a flow control equipment in a compressor has been found to give a substantial improvement in the compressor stable operational range. The experimental investigation has been performed with additional blades (of a fixed-geometry and adjustable types) in an axial-flow compressor stage. The fixed-geometry type additional blades were installed in the blade-to-blade duct of a rotor hub and in hub and tip zones of a guide vane. Total pressure diagrams for the stage embodiments (with and without the fixed-geometry additional blades) are presented. The adjustable tip additional blades were tested in two configurations, along the full length of the rotor blade chord projection, and located only in the inlet part of the rotor blade. This experimental investigation revealed a special importance of the inlet rotor part in rotating stall occurring.

Keywords: Compressor; Performance; Rotating stall; Additional blades

Nomenclature

b	–	blade chord, mm
$(b/t)_m$	–	rotor cascade solidity at the mean radius
$\bar{d}$	–	rotor hub/tip ratio
D_t	–	rotor tip (outer) diameter, mm
$\bar{h}$	–	rotor blade aspect ratio
$\bar{H}_{Td}$	–	design coefficient of theoretical head
$\Delta\bar{P}^0$	–	relative total pressure
ΔP_2^0	–	total pressure after the rotor
ΔP_{3avd}^0	–	averaged relative total pressure after the guide vane

[1]E-mail: nezym@mail.ru

r_c	–	current radius, mm
r_t	–	tip radius, mm
$\bar{r}$	–	relative radius
$\bar{r}_2$	–	relative radius after the rotor
$\bar{r}_3$	–	relative radius after the guide vane
S_a	–	axial clearance, mm
S_R	–	rotor tip clearance (absolute), mm
t	–	cascade space, mmm
U_t	–	tip circumferential velocity, m/s
ε_R	–	rotor blade camber angle, deg
c	–	current
ρ_1	–	flow density at the rotor inlet, kg/m^3
ϕ_d	–	design flow coefficient
ϕ_0	–	initial flow coefficient
ϕ_c	–	current flow coefficient
$\phi_{\max}$	–	maximum flow coefficient
ϕ_{or}	–	operational regime flow coefficient
ϕ_{sb}	–	stall boundary flow coefficient
0	–	IGV inlet, initial conditions
θ	–	rotor blade stagger angle, deg

Subscripts

1	–	R inlet
2	–	R outlet (GV inlet)
3	–	GV outlet
R	–	rotor
T	–	theoretical
a	–	axial
avd	–	averaged
d	–	design
m	–	mean
max	–	maximum
or	–	operational range
red	–	reduced
s	–	isentropic
sb	–	stall boundary
t	–	tip (outer)

Superscripts

0	–	total parameter

Abbreviations

AAB	–	adjustable additional blades
AB	–	additional blades

ATAB	–	adjustable tip additional blades
FGAB	–	fixed-geometry additional blades
GV	–	guide vane
H	–	rotor hub
IGV	–	inlet guide vane
L	–	(full) length
R	–	rotor
S	–	short (length)
T	–	rotor tip

1 Introduction

Jet engine manufacturers are continuously seeking to produce engines that are lighter and smaller in order to reduce manufacturing and operating costs. Part of the approach is to design a compressor with fewer stages while maintaining the required overall pressure rise and efficiency. A major limitation on the pressure rise in a subsonic axial-flow compressor stage is boundary layer separation on the blade suction surface and endwalls, i.e., hub and tip [1].

Flow control is a rather long-term technique for a turbomachine performance improvement. One method of mitigating the suction surface separation is to employ tandem airfoil blades [2–4]. The basic concept is that a new boundary layer forms on the second (aft) airfoil, allowing for high overall loading without the large flow separations that would be seen with a single airfoil.

The presence of a tip clearance between rotor blades and outer casing, S_R, (Fig. 1) is an integral part of compressor construction. The significant cause of compressor performance deterioration with time is the increase of blade tip clearance. This may result from erosion, by the atmospheric grit which is centrifuged to flow predominantly along the outer annulus wall, or by blade location problems.

Tip clearance loss in unshrouded blading is generally associated with the quantity of fluid leaking through a clearance (gap) between blade and casing. There are two main aspects of a tip clearance flow: one is blockage, which is a fluid dynamic effect and the other is loss, which is a thermodynamic effect. One of the effects is a vortex resulting from the scrubbing effect of the adjacent, moving blades, outer annulus wall and flow leakage through the blade tip clearance. Flow leakages are connected with the pressure differential at concave (increased pressure) and convex (decreased pressure) blade sides.

In general, in accordance with above-mentioned factors an air flow at the rotor blade tip is the most intricate in a stage at all. Unfavorable influence of tip clearance becomes apparent in decreasing of design head, efficiency and stable

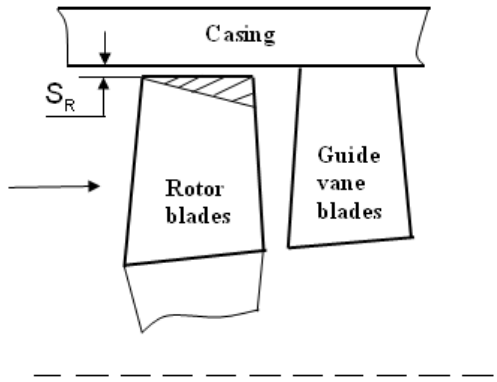

Figure 1: High-loss blade tip zone.

operation margin of a stage, and a compressor as a whole. Degree of this decreasing is connected with the stage geometric and kinematical parameters. Tip clearance effects are most severe when particularly short blades are used. One of a future-technology means of the tip clearance influence compensation is use of a casing treatment [5–10]. The other of various means of flow (boundary layer) control is use of fixed-geometry additional blades or additional guide vane in axial flow compressor stage duct.

2 Aerodynamic test of fixed-geometry additional blades in compressor stage

2.1 Experimental base

The aerodynamic test has been performed to investigate the fixed-geometry additional blades (FGAB) effect on a compressor stage performance. The test was conducted with a subsonic model axial compressor stage with rather curved profiles of the blades (the blade camber angle at the mean rotor radius, $\varepsilon_R \approx 60°$). It was supposed that dividing the blade-to-blade ducts by additional blades can prevent from the flow separation on the main blade wall, mainly because of a local diffusing effect decrease.

The special test facility was used to conduct the investigation. The tested stage has three cascades: inlet guide vane (IGV), rotor (R), and guide vane (GV). The principal parameters of the tested stage are given in Tab. 1.

Table 1: Principal parameters of the tested stage.

Parameter	Index	Dimension	Value
Design coefficient of theoretical head	$\bar{H}_{T_d}$	–	0.7
Design flow coefficient	ϕ_{d}	–	0.57
Reduced circumferential velocity	$U_{t_{red}}$	m/s	213
Rotor tip (outer) diameter	D_t	mm	400
Rotor hub/tip ratio	$\bar{d}$	–	0.9
Rotor blade aspect ratio	$\bar{h}$	–	1.0
Rotor cascade solidity at mean radius	$(\mathrm{b/t})_{\mathrm{m}}$	–	1.67

The tested configurations of the stage flow duct with all embodiments of the fixed-geometry additional blades location are shown in Fig. 2. The additional blades were manufactured from 0.25 mm thick steel sheet . They were located along the mean line of a blade-to-blade duct of the corresponding cascade. The outlet edge of any additional blade was located at the outlet front of the main cascade; the chord of such additional blade was less by 2 mm than the chord of the main blade. A hundred additional blades were manufactured for installation on the rotor hub, 10 – on the guide vane hub, and 10 – on the guide vane tip. The sector type of testing (meters were installed only in one circumferential sector) was used for the guide vane investigation.

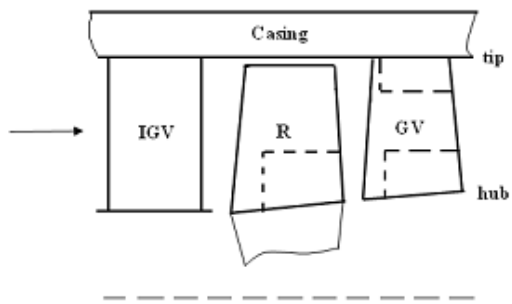

Figure 2: Configurations of the stage flow duct with all embodiments of the fixed-geometry additional blades: IGV – inlet guide vane, R – rotor, GU - guide vane.

The aerodynamic test was done at a reduced tip circumferential velocity at the rotor inlet $U_{t_{red}} \approx 125$ m/s. The performances of the whole stage (IGV+R+GV) and of the stage pack (IGV+R) were determined. The adiabatic head was deter-

mined with the help of the total pressure five-duct radial combs located before and after rotor cascade, and the theoretical head with the help of a torque measurement at a pendulous stator. The procedure of the total pressure measurement was accompanied by averaging of the pressure values along the cascade space and the blade height. The isentropic efficiency was determined with a precision about 0.5%.

Consequently there were obtained experimental diagrams (Fig. 3) of the relative (reduced to the inlet circumferential velocity head $\rho_1 U_t^2/2$ at the relative radius $\bar{r} = r_c/r_t$) total pressures after rotor (ΔP_2^0) and guide vane (ΔP_{3avd}^0). Test was performed with the flow coefficient $\phi \approx 0.715$. The total pressure after guide vanes was space averaged. On the grounds of these data the height of the fixed-geometry additional blades was chosen as a half of thickness of the layer occupied by deformed part of the pressure diagram.

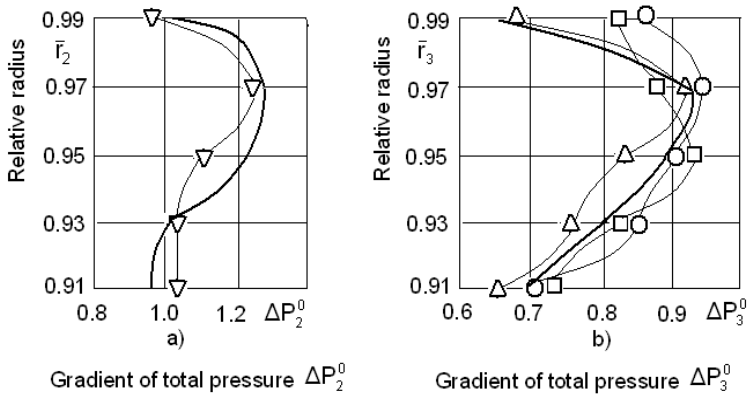

Figure 3: Diagrams of total pressure after rotor (a), after guide vane (b) of the stage: ——— – without AB, ▽ – with FGAB-R-H, □ – with FGAB-GV-T; △ – with FGAB-GV-H, ◯ – with FGAB-GV-T+H.

2.2 Experimental results

There were obtained the experimental results of separate tests with fixed-geometry additional blades (FGAB) on the rotor hub (FGAB-R+H), the guide vane tip (FGAB-GV-T), the guide vane hub (FGAB-GV-H) and on the guide vane tip and hub in combination (FGAB-GV-T+H). A comparison of the test performances without the additional blades and with three embodiments of additional blades in

the guide vane did not demonstrate any practical effect of the additional blades on the stage isentropic efficiency. In this case the coefficients of isentropic and theoretical heads were not practically changed. Such result is proved by rather similar likeness of the radial diagrams of the total pressure (Fig. 3). Thus, it may be supposed that a redistribution of the total pressure kept the whole integral pressure along the main blades height.

The location of the fixed-geometry additional blades on the rotor hub (FGAB-R-H) in the presence of FGAB on the guide vane tip and hub (FGAB-GV-T+H) did not change practically the performance of the pack (IGV+R). However it is rather interesting that in this case the diagram ΔP_2^0 (Fig. 3) in the rotor was smoothed and the total pressure level was decreased higher along the blade height. Simultaneously the radial diagram of the averaged total pressures after the guide vane was deformed significantly along the lower part of the main blades. Very likely that installation of the fixed-geometry additional blades in the rotor has eliminated a considerable hub flow separation which led to the flow acceleration at the tip part of the main blades. This fact promoted the flow separation from the suction surface of the main blade located above hub zone of the blade height.

3 Use of adjustable additional blades in compressor rotor

An increase in the tip clearance produces a substantial increase in leakage, which consequently produces a substantial loss in efficiency and stall margin. This invention [11] has proposed to locate additional blades only in the tip zone of an axial fan rotor (Fig. 4). The invention is directed to prevent the counter flow by providing guide vane disposed in the tip clearance and inclined symmetrically with the rotating blade, thereby to provide enhanced output flow rate and discharge pressure, as well as to reduce the level of noise.

The results of investigations of some adjustable additional tip blades are presented below. Tip elements of the rotor blades were removed totally or only in the inlet part of the main blades. Instead of the removed elements the cascades of adjustable additional (stator) blades (AAB) were installed with the possibility of the stagger angle adjusting. It was supposed that such tip device would change the conditions of a flow development at the compressor stage outer casing, delaying to some extent a boundary layer separation and rotating stall occurrence. Moreover, the adjustable additional blades located in the inlet part of blades may act as adjustable guide vane for the reminded rotor blade elements.

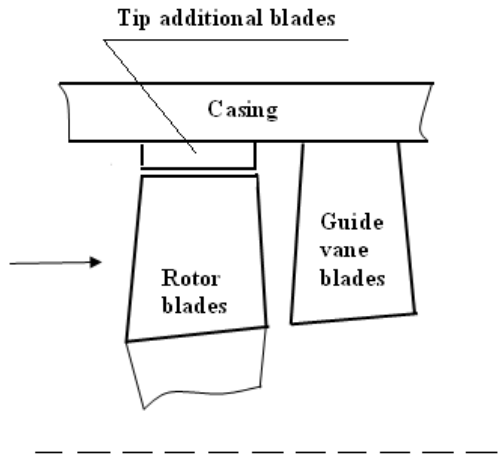

Figure 4: Tip additional blades.

3.1 Test base of investigations

The designs with long(at full length of the rotor chord projection) adjustable tip additional blades (ATAB-L), and with short (only in the inlet part) adjustable tip additional blades (ATAB-S) are shown in Fig. 5 in comparison with an original construction (without adjustable additional blades).

Additional blades were manufactured as framework from 2 mm thick steel sheet. Long blades, ATAB-L, had a chord of 25 mm and solidity 1.3. Short blades, ATAB-S, were manufactured as plates (240 pieces) with a chord of 7 mm (28% of the rotor blade chord) and the same solidity 1.3. The additional blade height in both configurations was 13% of the rotor blade height, a radial clearance between additional and rotor blades was in the limits of 3.9–3.2% of the inlet duct height. Moreover inlet edges of additional blades were sharpened.

The model test compressor stage with outer diameter $D_t = 400$ mm, hub/tip ratio $\bar{d}_1 = 0.85$ was used for the investigation. The stage was tested without inlet guide vane and under the condition that the velocity is equal to 0.65 of the design tip circumferential velocity value. Thus, the stage rotor operated at substantially off-design regimes with respect to the inlet conditions and rotational speed.

The stage rotor performance and stall margin were determined. The adiabatic head was measured with the help of the total pressure five-duct radial combs located before and after the rotor cascade, the theoretical head was determined with the help of the torque measurement at a pendulous stator. The principal tests

have been founded on the comparison of the flow coefficients specifying a location of a stall boundary, ϕ_{sb}, and a maximum flow rate, $\phi_{\max}$. The corresponding operational range, ϕ_{or}, of the rotor performance was determined as follows:

$$\phi_{or} = \frac{\phi_{\max} - \phi_{sb}}{\phi_{sb}} \times 100\% \ . \tag{1}$$

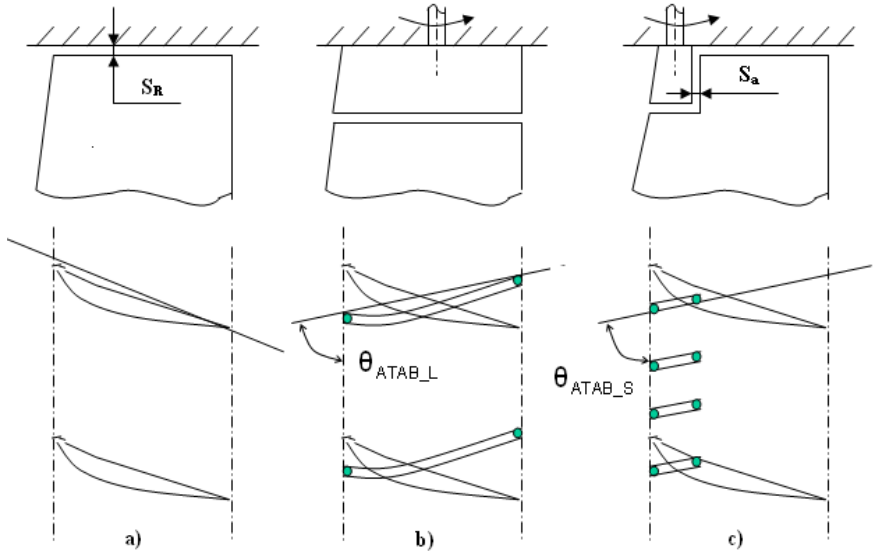

Figure 5: Tested devices: a) origin design, b) long ajustable tip additional blades, c) short adjustable tip additional blades.

The data obtained with the additional blades, ϕ_i, were compared with the corresponding data of the original design, ϕ_0, with the initial rotor tip clearance $S_R = 0.45$ mm (the relative tip clearance 1.45%) as follows:

$$\Delta\phi_c = \frac{\phi_c - \phi_0}{\phi_0} \times 100\% \ . \tag{2}$$

The accuracy of the rotor test determination was estimated to be near 0.5%, of the flow coefficients – near 1%.

3.2 Results of investigation

While investigations of the long tip additional blades (ATAB-L) the stagger angle of the additional blades was changing in the range from 40° to 70°. As a result,

the rotor performance was shifted significantly (at 13–20%) to the side of the less flow coefficients. This phenomenon was accompanied by decrease of the rotor efficiency by more than 30% because of significant energy loss in the ATAB-L zone. The maximum extension of the stage operational range was 18%. Thus, the substitution of an entire tip part of the rotor blades for the adjustable tip additional blades (ATAB-L) was accompanied by a considerable extension of the stage operational range together with a sharp efficiency drop. Investigations of the short additional blades (AAB-S) have been carried out in two stages.

Firstly, the rotor performances were determined under changes of ATAB-S stagger angles θ_{ATAB-S} from 30° to 50° and an axial clearance, S_a, from 1 to 5 mm. At the initial axial clearance, $S_a = 1$ mm, the maximum shift of the stall boundary to the less flow coefficients (near 15%) and the extension of the operational range (17%) were obtained at the ATAB-S stagger angle about 45°. An axial location of ATAB-S was effecting very significantly on the stall boundary margin. In particular in the range of 1, 3, and 5 mm of the axial clearance, the maximum positive effect of the stall boundary shift (24%) and operational range extension (42%) were observed at S_a= 3 mm and $\theta_{ATAB-S} = 45°$.

Note that in all ATAB-S investigations a point of maximum flow coefficient was shifted to the left side of the rotor performance (by approximately 12%). This fact may be useful for a cascade design. However, the head coefficients (especially the adiabatic head) were decreased significantly causing the corresponding decrease of the rotor efficiency. However, this effect was not so great as in the case of the ATAB-L testing.

On the grounds of the results of the short additional blades investigation (in the inlet part of the rotor cascade) it has been possible put forward two assumptions:

- an inlet tip zone of rotor blades is especially important for a rotating stall occurrence,
- an optimization of flow in the remanded blade elements may be executed by adjusting the additional blades stagger angles.

At the second stage of the investigations, the remained elements of the rotor blades were sharpened in the inlet parts. This procedure permitted to considerably decrease the energy loss in the tip zone of the rotor blades, hence to compensate the decrease of the adiabatic head coefficients and the rotor efficiency. Therefore, the effect of an extension of the operational range was conserved too. Thus, in the variant of $\theta_{ATAB-S} = 30°$ and $S_a = 1$ mm the isentropic efficiency was decreased only at 2.5% (for comparison, it was decreased at 19.5% in the variant without a sharpening procedure).

4 Conclusions

1. The results of the aerodynamic test showed that installation of fixed-geometry additional blades on the hub of a compressor rotor may effect significantly on a flow in the hub zone preventing the flow separation in this field. Correspondingly it is possible to influence effectively upon the flow in an axial-flow compressor stage of an increased aerodynamic loading. However it is necessary to carry out further investigations for optimization the design parameters of additional blades.
2. Adjustable additional tip blades located along full length of the tip chord projection of a rotor blade are less effective for a compressor performance improvement in comparison with the similar blades located only in the inlet part of the rotor cascade.
3. Installation of adjustable tip additional blades in the inlet part of a rotor cascade may effectively influence on a flow in the tip zone. Optimally changing stagger angle and axial location of sharpened blades it is rather likely to extent significantly an axial-flow compressor stage operational range without a great drop of efficiency.

Received 20 July 2015, revised form 19 April 2016

References

[1] Koch C.C., Smith L.H.Jr.: *Loss sources and magnitudes in axial-flow compressors.* In: ASME Paper 75-Wa/GT-6 (1975), 14.

[2] Bammert K., Beelte. H.: *Investigation of an axial compressor with tandem cascades.* J. Eng. Power, Trans. ASME **102**(1980), 4, 971–977.

[3] Wu C.H., Zhuang B., Guo B.: *Experimental investigation of tandem blade cascades UIT double-circular arc profiles.* ASME Paper 85-GT-94 (1985), 7.

[4] Nezym V.Yu., Gomez-Mancilla J., Korkishko S.V.: *Statistical model for turning angle determination of compressor tandem cascade.* Proc. ISROMAC-10 (2004), 6.

[5] Greitzer E.M., Nikkanen J.P., Haddad D.E., Mazzawy R.S., Joslin H.D.: *A fundamental criterion for the application of rotor casing treatment.* J. Fluids Eng., Trans. ASME **101**(1979), 1, 237–243.

[6] Smith G.D. Jr., Cumpsty N.A.: *Flow phenomena in compressor casing treatment.* J. Eng. Gas Turb. Power, Trans. ASME **106**(1984), 3, 532–541.

[7] Fujita H., Takata H.: *A study on configurations of casing treatment for axial flow compressors.* JSME Bull. **230**(1984), 27, 1675–1681.

[8] Bae J., Breuer K.S., Tan C.S.: *Control of tip clearance flows in axial compressors.* Proc. AIAA Fluids 2000 Conference & Exhibit (2000), 1–11.

[9] Nezym V.Yu.: *Parametric investigation of casing treatment influence on compressor stable operation.* Exp. Therm. Fluid Sci. **29**(2004), 2, 209–215.

[10] Nezym V.Yu.: *A statistical model for the effect of casing treatment recess on compressor rotor performance.* Exp. Therm. Fluid Sci. **31**(2007), 1, 203–214.

[11] Honda J. *et al.*: *Axial fan.* United States Patent, 4152094 (1979), 13.